Christiane Stoll, David van Gerven and Hubert Huppertz*

# Serendipitous formation of $K_{15}NaSn_5F_{36}$

https://doi.org/10.1515/znb-2019-0201
Received November 30, 2019; accepted December 27, 2019

**Abstract:** $K_{15}NaSn_5F_{36}$ crystallizes in the hexagonal crystal system with space group $P6_3/m$ and lattice parameters of $a = 1060.3(2)$ and $c = 2011.9(4)$ pm. The unit-cell volume amounts to 1.9588(7) nm³. Its fundamental building blocks are quasi-isolated $[SnF_6]^{2-}$ and $[NaF_6]^{5-}$ octahedra, which are imbedded into a matrix of potassium cations. Within the structure, these units form a layer-like arrangement consisting either of mixed $[SnF_6]^{2-}/[NaF_6]^{5-}$ or pure $[SnF_6]^{2-}$ layers. The structural model was further confirmed by BLBS and CHARDI calculations.

**Keywords:** crystal structure; FT-IR spectroscopy; potassium sodium fluoridostannate.

## 1 Introduction

Fluorides are a versatile class of compounds, offering 0-dimensional to 3-dimensional structural motifs. The fundamental building blocks may consist of tetrahedral up to nonahedral units [1, 2]. Among these, the octahedral coordination sphere is one of the most commonly observed structural motifs [1, 3]. These entities can not only occur isolated, but also connected *via* common corners, edges, or faces [1, 3]. This can lead to the formation of quasi-isolated structural units, chains, or networks [1]. Most prominent representatives of the fluorides are the hexafluoridometallates $A_2MF_6$ ($A$ = monovalent cation, $M$ = tetravalent cation), $A_3M'F_6$ ($M'$ = trivalent cation), and $A'MF_6$ ($A'$ = divalent cation) [1], in which quasi-isolated octahedral $MF_6$ building blocks dominate the solid state structures. Recently, hexafluoridosilicates like $K_2SiF_6$ or $Li_2SiF_6$ exhibiting quasi-isolated octahedral units received a lot of attention as host materials for $Mn^{4+}$. Ever since $K_2SiF_6$:$Mn^{4+}$ was adopted as a red luminescent material in white light emitting diodes, numerous novel hexafluoridometallate phosphors have been discovered [4–6]. However, within the group of tin fluorides not only the hexafluoridostannates are known, but also compositions like $ASn_2F_5$ ($A$ = monovalent cation), $KSnF_3$, $A'SnF_4$ ($A'$ = divalent cation), $A''SnF_7$ ($A''$ = trivalent cation), or $Na_4Sn_3F_{10}$ have been mentioned in the literature [7–17]. Nearly all of the published fluoridostannates contain tin in the oxidation state 2+. Therefore, these structures commonly exhibit a square pyramidal coordination of tin, which leaves space for the lone pair of electrons. The oxidation state of 4+ is only observed within the hexafluoridostannates like $Cs_2SnF_6$, $KNaSnF_6$, $RbNaSnF_6$, and $CsNaSnF_6$, and within $A''SnF_7$ ($A''$ = trivalent cation) [11, 18, 19]. These materials containing $Sn^{4+}$ show an octahedral coordination sphere around the tin atom. Interestingly, materials with large cell parameters containing solely isolated octahedral units are only mentioned scarcely. One example is $(NH_4)_3SnF_7$, which crystallizes in the cubic crystal system with the cell parameter $a = 1208.6(1)$ pm and a volume of 1.765 nm³ [20]. Here, we took the chance to characterize $K_{15}NaSn_5F_{36}$, which also exhibits an unusually large unit cell (hexagonal, $a = 1060.3(2)$, $c = 2011.9(4)$ pm, $V = 1.9588(7)$ nm³), whilst containing only simple but uniquely arranged building blocks.

## 2 Experimental section

### 2.1 Synthesis

$K_{15}NaSn_5F_{36}$ was synthesized in welded copper ampoules. $KHF_2$ and $SnO_2$ (Strem Chemicals, Newburyport, USA, 99.9%) were ground together in an agate mortar with a molar ratio of 3:1 under argon atmosphere (glove box, MBraun Inertgas-System GmbH, Germany). The powder was then transferred into copper ampoules, which were welded in a miniaturized arc-welding installation (further information on the arc-welding installation can be retrieved from [21]). The closed ampoule was subsequently transferred into a silica glass ampoule, which was filled with 400 mbar argon atmosphere, placed into a tube furnace and heated up to $T = 300$°C with a heating rate of 3 K min⁻¹. The temperature was kept at 300°C for 96 h and subsequently cooled to 250°C at a cooling rate of 0.1 K min⁻¹. This temperature was kept for another 24 h

***Corresponding author: Hubert Huppertz,** Institut für Allgemeine, Anorganische und Theoretische Chemie, Universität Innsbruck, Innrain 80–82, 6020 Innsbruck, Austria,
e-mail: hubert.huppertz@uibk.ac.at
**Christiane Stoll:** Institut für Allgemeine, Anorganische und Theoretische Chemie, Universität Innsbruck, Innrain 80–82, 6020 Innsbruck, Austria
**David van Gerven:** Institut für Anorganische Chemie, Universität zu Köln, Greinstraße 6, 50939 Köln, Germany

and followed by cooling to 100°C at a cooling rate of 0.1 K $min^{-1}$. Subsequently, the furnace was turned off and the sample was quenched to room temperature. A colourless crystalline material was recovered, from which a single crystal of $K_{15}NaSn_5F_{36}$ could be isolated. The incorporated sodium in the compound originates from the starting material $KHF_2$ contaminated by sodium. As only a few single crystals could be isolated under oil (Fomblin) no EDX analysis was possible. The presence of sodium is not unexpected, as it has been observed in a number of crystals of samples prepared with the contaminated educt $KHF_2$. As is shown below, the shorter Na–F bonds in comparison to the K–F bonds, as well as the difference in electron density of sodium in contrast to potassium, clearly show the presence of sodium (Na1 site).

First attempts to synthesize bulk samples of $K_{15}NaSn_5F_{36}$ by solid-state synthesis have not been successful as yet.

## 2.2 X-ray analysis

The analysis of the crystal was carried out at the P24 Beamline of the PETRA III facility at DESY Hamburg (Germany). For the analysis, a single crystal was mounted onto a Huber 4-circle Kappa-diffractometer. The synchrotron radiation was monochromatized by a water-cooled double crystal monochromator [Si(111), Si(311)] to yield a wavelength of $\lambda = 0.47686$ Å. The collected intensity data were reduced, and a cell refinement was carried out with the help of XDS (Version March 15, 2019, W. Kabsch, MPI Heidelberg). On the basis of the extinction conditions, the space groups $P6_3/m$ (no. 176), $P6_3$ (no. 173), and $P6_322$ (no. 182) were considered for the structure solution (SHELXS-98 [22]) and refinement. The centrosymmetric space group $P6_3/m$ (no. 176) was found to be correct.

A refinement in space group $P6_3$, which lacks the additional mirror plane of $P6_3/m$, is possible but does not lead to better $R$ values. In space group $P6_3$ residual electron density is distributed equally for both possible sites of K4 in an approximate ratio of 1:1. As no suitable twinning model was found either, we believe that the crystal structure of $K_{15}NaSnF_{36}$ is best described in the centrosymmetric space group $P6_3/m$.

The parameter refinement (full-matrix least-squares against $F^2$) was carried out with SHELXL-2013 [22, 23] as implemented in the WINGX-2013.3 suite [24]. The anisotropic refinement led to values of 0.0291 and 0.0631 for $R1$ and $wR2$ (all data), respectively.

Further information on the crystal structure investigation can be obtained from the joint CCDC/FIZ Karlsruhe deposition service on quoting the deposition number CCDC 1968496 for $K_{15}NaSn_5F_{36}$.

# 3 Results and discussion

$K_{15}NaSn_5F_{36}$ crystallizes in the hexagonal crystal system with space group $P6_3/m$ (no. 176). Its lattice parameters are 1060.3(2) and 2011.9(4) pm for $a$ and $c$, respectively. The unit cell contains 114 atoms. This equals two formula units. Therefore, the Pearson code of $K_{15}NaSn_5F_{36}$ is $hP114$. The asymmetric unit of $K_{15}NaSn_5F_{36}$ consists of two tin, four potassium, one sodium, and seven fluorine positions. K1, K2, F1, F3, F5, F6, and F7 are located on the general Wyckoff positions 12*i*. Sn1, F2, and F4 are located at the special Wyckoff positions 6*h*, Sn2 and K4 (site occupancy factor (SOF) = 0.5) at the special Wyckoff positions 4*f*, K3 at 4*e*, and Na1 is located at 2*b*. Therefore, the Wyckoff sequence of $K_{15}NaSn_5F_{36}$ is $i^7h^3f^2eb$. Information about the crystal structure refinement is listed in Table 1. Further information about atomic coordinates, displacement parameters, as well as selected interatomic distances and angles are shown in Tables 2–5.

**Table 1:** Crystal data and structure refinement of $K_{15}NaSn_5F_{36}$.

| | |
|---|---|
| Empirical formula | $K_{15}NaSn_5F_{36}$ |
| Molar mass, g $mol^{-1}$ | 1886.94 |
| Crystal system | Hexagonal |
| Space group | $P6_3/m$ (no. 176) |
| Single-crystal diffractometer | Kappa-diffractometer, P24 Beamline, DESY Hamburg |
| Radiation/wavelength $\lambda$, Å | Synchrotron/0.47686 |
| $a$, pm | 1060.3(2) |
| $c$, pm | 2011.9(4) |
| $V$, $nm^3$ | 1.9588(7) |
| Formula units per cell, $Z$ | 2 |
| Calculated density, g $cm^{-3}$ | 3.20 |
| Temperature, K | 293(2) |
| Absorption coefficient, $mm^{-1}$ | 1.2 |
| $F$(000), e | 1740 |
| $2\theta$ range, ° | 3.0–39.2 |
| Range in $hkl$ | ±14, ±14, ±28 |
| Total no. of reflections | 17486 |
| Independent reflections/ref. parameters/$R_{int}$ | 1956/94/0.0328 |
| Reflections with $I > 2\sigma(I)$ | 1941 |
| Goodness-of-fit on $F_i^2$ | 1.269 |
| Absorption correction | Semi-empirical (from equivalents) |
| Final $R1/wR2$ [$I > 2\sigma(I)$] | 0.0289/0.0630 |
| Final $R1/wR2$ (all data) | 0.0291/0.0631 |
| Largest diff. peak/hole, e $Å^{-3}$ | 1.89/−1.34 |

**Table 2:** Wyckoff positions, atomic coordinates, and equivalent isotropic displacement parameters $U_{eq}$ (Å²) of $K_{15}NaSn_5F_{32}$.

| Atom | Wyckoff position | *x* | *y* | *z* | $U_{eq}$ | SOF |
|---|---|---|---|---|---|---|
| Sn1 | 6*h* | 0.67422(3) | 0.02271(4) | 1/4 | 0.0143(2) | 1 |
| Sn2 | 4*f* | 1/3 | 2/3 | 0.48491(2) | 0.0127(2) | 1 |
| K1 | 12*i* | 0.37344(9) | 0.0306(2) | 0.35517(4) | 0.0234(2) | 1 |
| K2 | 12*i* | 0.28172(8) | 0.29443(7) | 0.44846(3) | 0.0162(2) | 1 |
| K3 | 4*e* | 0 | 0 | 0.34055(5) | 0.0140(2) | 1 |
| K4 | 4*f* | 1/3 | 2/3 | 0.1917(2) | 0.0188(4) | 0.5 |
| Na1 | 2*b* | 0 | 0 | 1/2 | 0.0082(5) | 1 |
| F1 | 12*i* | 0.6785(3) | 0.1503(3) | 0.3218(2) | 0.0387(6) | 1 |
| F2 | 6*h* | 0.4589(3) | 0.9229(3) | 1/4 | 0.0188(5) | 1 |
| F3 | 12*i* | 0.6721(3) | 0.8901(3) | 0.1816(2) | 0.0308(5) | 1 |
| F4 | 6*h* | 0.8905(3) | 0.1243(3) | 1/4 | 0.0217(6) | 1 |
| F5 | 12*i* | 0.4017(3) | 0.8386(2) | 0.4267(2) | 0.0302(5) | 1 |
| F6 | 12*i* | 0.5093(2) | 0.7803(3) | 0.5375(2) | 0.0285(5) | 1 |
| F7 | 12*i* | 0.1756(2) | 0.0071(2) | 0.43355(9) | 0.0131(3) | 1 |

$U_{eq}$ is defined as one third of the trace of the orthogonalized $U_{ij}$ tensor (standard deviations in parentheses).

**Table 3:** Anisotropic displacement parameters $U_{ij}$ in Å² (standard deviations in parentheses).

| Atom | $U_{11}$ | $U_{22}$ | $U_{33}$ | $U_{12}$ | $U_{13}$ | $U_{23}$ |
|---|---|---|---|---|---|---|
| Sn1 | 0.0105(2) | 0.0222(2) | 0.0102(2) | 0.0081(2) | 0 | 0 |
| Sn2 | 0.0089(2) | 0.0088(2) | 0.0203(2) | 0.00443(6) | 0 | 0 |
| K1 | 0.0269(4) | 0.0397(4) | 0.0158(3) | 0.0257(3) | 0.0065(3) | 0.0073(3) |
| K2 | 0.0178(3) | 0.0126(3) | 0.0184(3) | 0.0076(2) | 0.0007(2) | 0.0006(2) |
| K3 | 0.0160(3) | 0.0160(3) | 0.0100(4) | 0.0080(2) | 0 | 0 |
| K4 | 0.0188(6) | 0.0188(6) | 0.019(2) | 0.0094(3) | 0 | 0 |
| Na1 | 0.0098(7) | 0.0098(7) | 0.005(2) | 0.0049(4) | 0 | 0 |
| F1 | 0.022(2) | 0.048(2) | 0.041(2) | 0.014(2) | −0.003(2) | −0.023(2) |
| F2 | 0.012(2) | 0.022(2) | 0.019(2) | 0.006(2) | 0 | 0 |
| F3 | 0.038(2) | 0.044(2) | 0.021(2) | 0.028(2) | −0.0051(9) | −0.013(2) |
| F4 | 0.011(2) | 0.028(2) | 0.026(2) | 0.010(2) | 0 | 0 |
| F5 | 0.028(2) | 0.024(2) | 0.038(2) | 0.0124(9) | −0.002(1) | 0.013(2) |
| F6 | 0.017(2) | 0.028(2) | 0.036(2) | 0.0077(8) | −0.0087(9) | −0.0030(9) |
| F7 | 0.0126(8) | 0.0135(8) | 0.0134(8) | 0.0066(7) | 0.0007(6) | −0.0008(6) |

**Table 4:** Interatomic distances in pm (standard deviations in parentheses).

| | | | | | | | | |
|---|---|---|---|---|---|---|---|---|
| Sn1–F3 | 195.9(2) | 2× | Sn2–F6 | 195.1(2) | 3× | Na1–F7 | 226.3(2) | 6× |
| –F1 | 196.3(2) | 2× | –F5 | 197.4(2) | 3× | **Ø** | **226.3** | |
| –F2 | 197.9(3) | | **Ø** | **196.3** | | | | |
| –F4 | 198.7(3) | | | | | | | |
| **Ø** | **196.8** | | | | | | | |
| K1–F7 | 253.5(2) | | K2–F7 | 267.4(2) | | K3–F7 | 261.4(2) | 3× |
| –F5 | 263.0(2) | | –F7 | 267.6(2) | | –F4 | 281.7(2) | 3× |
| –F2 | 276.3(2) | | –F7 | 268.5(2) | | –F3 | 309.7(3) | 3× |
| –F6 | 278.1(3) | | –F6 | 271.5(2) | | **Ø** | **284.3** | |
| –F1 | 279.9(3) | | –F3 | 277.0(3) | | | | |
| –F3 | 281.8(3) | | –F6 | 279.1(3) | | K4–F2 | 263.0(3) | 3× |
| –F1 | 290.2(3) | | –F5 | 282.4(2) | | –F5 | 286.4(3) | 3× |
| –F4 | 293.4(2) | | –F1 | 317.2(3) | | –F3 | 317.0(3) | 3× |
| **Ø** | **277.0** | | **Ø** | **278.8** | | **Ø** | **288.8** | |

**Table 5:** Bond angles in deg (standard deviations in parentheses).

| | | |
|---|---|---|
| F3–Sn1–F1 177.2(2) 2× | F3–Sn1–F3 89.2(2) | F6–Sn2–F6 93.4(2) 3× |
| F2–Sn1–F4 179.6(2) | F3–Sn1–F1 88.0(2) 2× | F6–Sn2–F5 87.4(2) 3× |
| **Ø$_{180}$ 178.0** | F1–Sn1–F1 94.7(2) | F6–Sn2–F5 90.7(2) 3× |
| | F3–Sn1–F2 91.2(2) 2× | F5–Sn2–F5 88.4(2) 3× |
| | F1–Sn1–F2 89.5(1) 2× | **Ø$_{90}$ 90.0** |
| | F3–Sn1–F4 89.1(2) 2× | |
| F6–Sn2–F5 175.8(2) 3× | F1–Sn1–F4 90.2(1) 2× | |
| **Ø$_{180}$ 175.8** | **Ø$_{90}$ 90.0** | |
| F7–Na2–F7 180 3× | F7–Na2–F7 88.64(7) 5× | |
| **Ø$_{180}$ 180** | F7–Na2–F7 91.36(7) 5× | |
| | **Ø$_{90}$ 90.0** | |

The main structural motifs of $K_{15}NaSn_5F_{36}$ are quasi-isolated $[SnF_6]^{2-}$ and $[NaF_6]^{5-}$ octahedra (Fig. 1). Within the two different $[SnF_6]^{2-}$ octahedra the Sn–F bond lengths vary from 195.1(2) to 198.7(3) pm (Table 4). This is in accordance with the value given for $Cs_2SnF_6$ in the literature ($d_{Sn-F}$ = 195.2 pm) [25]. The bond angles confirm a distorted octahedral coordination sphere for both, Sn1 and Sn2 (Table 5). Sodium, in contrast, experiences a nearly perfect octahedral coordination sphere with Na–F bond lengths of 226.3(2) pm and angles close to 90° (Table 5). The bond length is in accordance with the Na–F bond length of 231.7 pm in NaF [26].

These octahedral units are imbedded into a matrix of potassium cations. Within the structure, there are four crystallographically different potassium positions. The corresponding coordination spheres are depicted in Fig. 2. The K–F bond lengths vary between 253.5(2) and 317.2(3) pm. It is noteworthy that the site occupancy of K4 is only 0.5. This is likely a result of a statistical disorder at this site. Around the K4 sites (Fig. 3, K4_A and K4_B created by symmetry operations), a coordination sphere is built up, which is surrounded solely by $[SnF_6]^{2-}$ units (Fig. 3). In comparison, all other potassium cation positions are coordinated by a mixture of $[SnF_6]^{2-}$ and $[NaF_6]^{5-}$ units, which does not leave enough space for a disorder on these sites. Therefore, just one of the positions K4_A or K4_B is occupied, with a probability of 50% for each option.

$K_{15}NaSn_5F_{36}$ exhibits a layer-like arrangement. Layer one (L1) consists of a mixture of quasi-isolated $[SnF_6]^{2-}$ and $[NaF_6]^{5-}$ octahedra (Fig. 4, marked blue), whereas layer two (L2) consists solely of quasi-isolated $[SnF_6]^{2-}$ octahedra (Fig. 4, marked green). These layers are stacked along the crystallographic *c* axis (Fig. 4, top). Within every second layer of L1 the orientation of the octahedral units changes, like mirrored on (110). Additionally, every second layer of L2 is turned around the *c* axis by 180°.

The structural model was confirmed by bond-length/bond-strength (BLBS) [27, 28] and charge-distribution (CHARDI, program CHARDI2015) [29, 30] calculations (Table 6). At the site K4, the CHARDI calculations predict a charge of +0.48. This is in accordance with the structural data, as the SOF of K4 is 0.5. In contrast, the site occupancy cannot be taken into account during the BLBS calculations. This leads to a calculated charge of +0.90 for K4.

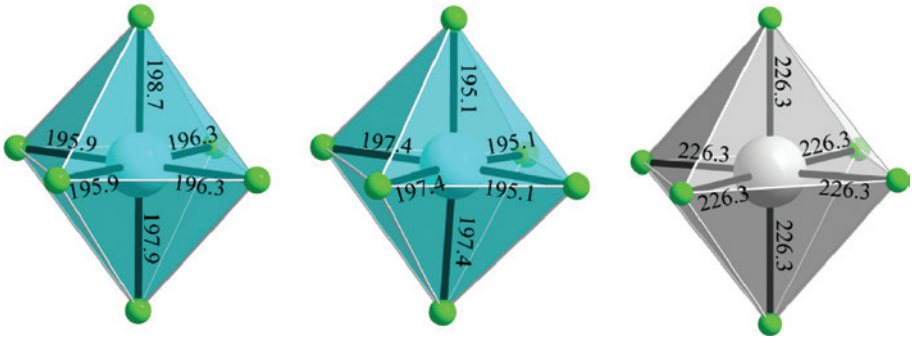


**Fig. 1:** Main structural motifs of $K_{15}NaSn_5F_{36}$. The octahedral coordination spheres of Sn1, Sn2, and Na1 are shown on the left, center, and right, respectively. Bond lengths are given in pm.

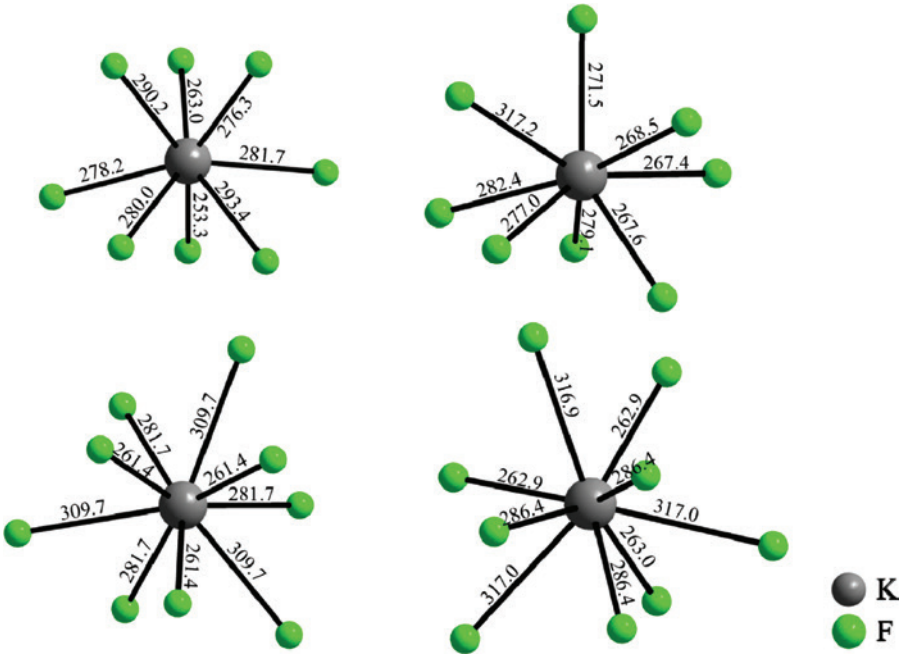


**Fig. 2:** Coordination spheres of K1 (top, left), K2 (top, right), K3 (bottom, left), and K4 (bottom, right). Bond lengths are given in pm.

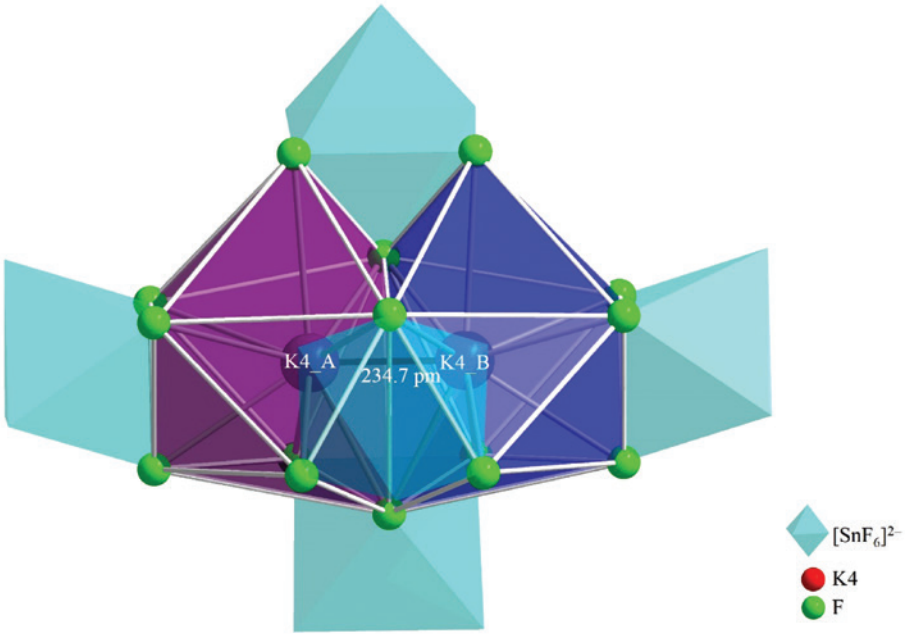


**Fig. 3:** Coordination sphere around the K4 position. Either K4_A or K4_B is occupied.

## 4 Conclusion

$K_{15}NaSn_5F_{36}$ was characterized by means of single-crystal structure determination. It is, next to $KNaSnF_6$, the second representative in the class of potassium sodium fluoridostannates [19]. $K_{15}NaSn_5F_{36}$ exhibits its own structure type, showing quasi-isolated $[SnF_6]^{2-}$ and $[NaF_6]^{5-}$ entities that are imbedded into a matrix of potassium cations, which leads to an unusually large unit cell. One of the potassium positions shows a statistical disorder, because of a large void created by four $[SnF_6]^{2-}$ octahedra. The structural model was confirmed by BLBS and CHARDI calculations. Crystals of $K_{15}NaSn_5F_{36}$ therefore have a large unit cell with an unusually high alkali metal to tin ratio

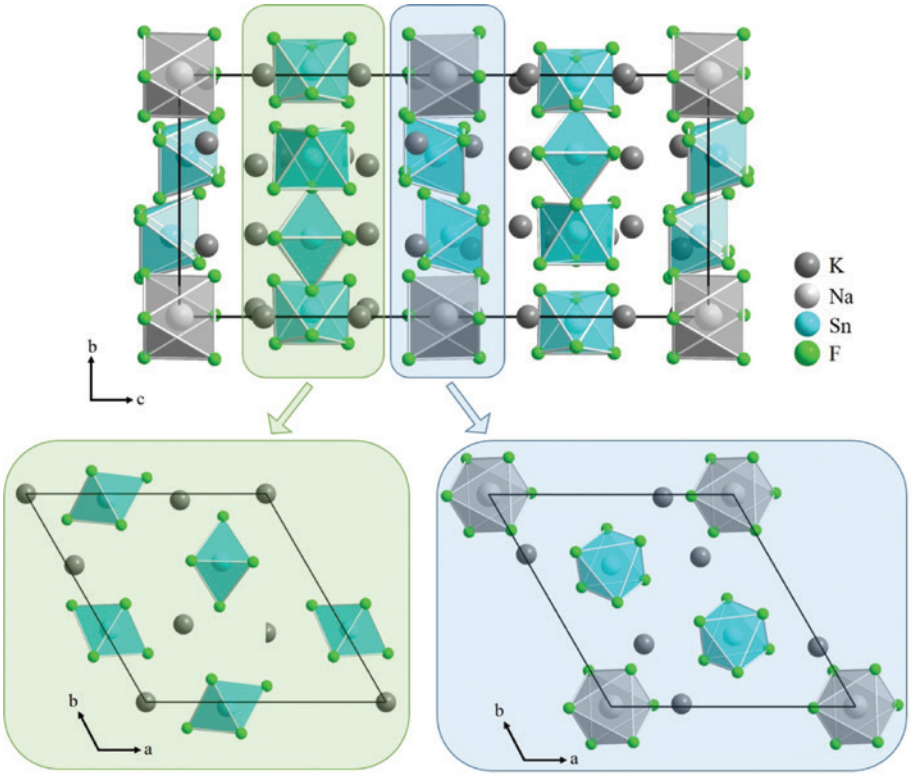


**Fig. 4:** Crystal structure projection of $K_{15}NaSn_5F_{36}$ along [100] (top, unit cell in solid black). Layers consisting of $[SnF_6]^{2-}$ and $[NaF_6]^{5-}$ units are marked in blue, layers consisting solely of $[SnF_6]^{2-}$ are marked in green. Two examples of layers depicted along [00$\bar{1}$] are shown at the bottom.

**Table 6:** Values of the charge contributions according to both the bond-valence sums (∑V) and the CHARDI (∑Q) concept.

| | Sn1 | Sn2 | K1 | K2 | K3 | K4 | Na1 |
|---|---|---|---|---|---|---|---|
| BLBS | +4.24 | +4.31 | +1.04 | +1.00 | +0.98 | +0.90 | +1.23 |
| CHARDI | +4.09 | +3.90 | +1.01 | +0.99 | +1.00 | +0.48 | +1.00 |
| | **F1** | **F2** | **F3** | **F4** | **F5** | **F6** | **F7** |
| BLBS | −0.96 | −1.29 | −1.05 | −1.04 | −1.07 | −1.12 | −1.09 |
| CHARDI | −0.91 | −1.08 | −0.99 | −1.01 | −0.98 | −1.08 | −1.00 |

of 3:1 (K:Sn). Additionally, this substance, if accessible as bulk material, might qualify as host material for doping with $Mn^{4+}$ to yield a red phosphor, as it shows the preferable octahedral coordination sphere around the metal cations.

**Acknowledgments:** We acknowledge DESY (Hamburg, Germany), a member of the Helmholtz Association HGF, for the provision of experimental facilities. Parts of this research were carried out at PETRA III and we would like to thank Carsten Paulmann and Heiko Schulz-Ritter for assistance in using the Kappa-diffractometer. Special thanks go to Prof. Dr. Mathias Wickleder and his research group for the isolation of the single crystal and the collection of the data at DESY. We also want to express our gratitude to Prof. Dr. Klaus Wurst for the help with the single-crystal structure refinement. For financial support of this work, we want to thank OSRAM Opto Semiconductors GmbH.

## References

[1] M. Leblanc, V. Maisonneuve, A. Tressaud, *Chem. Rev.* **2015**, *115*, 1191–1254.
[2] M. Leblanc, A. Tressaud, *Fluorides and Oxide-Fluorides of d-Transition Elements*, in *Comprehensive Inorganic Chemistry II: From Elements to Applications* (2nd edition) (series Eds.: J. Reedijk, K. R. Poeppelmeier), Vol. 2, *Transition Elements, Lanthanides and Actinides* (Eds.: E. V. Antipov, A. M. Abakumov, A. V. Shevelkov), Elsevier, Amsterdam, **2013**, pp. 161–185.
[3] W. Massa, D. Babel, *Chem. Rev.* **1988**, *88*, 275–296.
[4] S. Adachi, *J. Lumin.* **2018**, *197*, 119–130.
[5] T. Takahashi, S. Adachi, *J. Electrochem. Soc.* **2008**, *155*, E183–E188.
[6] C. Stoll, J. Bandemehr, F. Kraus, M. Seibald, D. Baumann, M. J. Schmidberger, H. Huppertz, *Inorg. Chem.* **2019**, *58*, 5518–5523.

[7] R. Kanno, S. Nakamura, K. Ohno, Y. Kawamoto, *Mat. Res. Bull.* **1991**, *26*, 1111–1117.
[8] J. D. Foulon, J. Durand, A. Larbot, L. Cot, *Eur. J. Solid State Inorg. Chem.* **1993**, *30*, 87–99.
[9] O. Graudejus, B. G. Müller, *Z. Anorg. Allg. Chem.* **1996**, *622*, 1601–1608.
[10] S. Vilminot, R. Bachmann, H. Schulz, *Solid State Ionics* **1983**, *9 & 10*, 559–562.
[11] O. Graudejus, F. Schrötter, B. G. Müller, R. Hoppe, *Z. Anorg. Allg. Chem.* **1994**, *620*, 827–832.
[12] R. R. McDonald, A. C. Larson, D. T. Cromer, *Acta Crystallogr.* **1964**, *17*, 1104–1108.
[13] G. Bergerhoff, L. Goost, *Acta Crystallogr.* **1970**, *B26*, 19–23.
[14] Y. V. Kokunov, D. G. Detkov, Y. E. Gorbunova, M. M. Ershova, Y. N. Mikhailov, *Dokl. Chem.* **2001**, *376*, 52–54.
[15] M. M. Ahmad, K. Yamada, *J. Chem. Phys.* **2007**, *127*, 124507.
[16] P. Berastegui, S. Hull, S. G. Eriksson, *J. Solid State Chem.* **2010**, *183*, 373–378.
[17] T. Thao Tran, P. Shiv Halasyamani, *J. Solid State Chem.* **2014**, *210*, 213–218.
[18] A. V. Gerasimenko, S. B. Ivanov, T. F. Antokhina, V. I. Sergienko, *Koord. Khim.* **1992**, *18*, 1139–1143.
[19] A. V. Gerasimenko, S. B. Ivanov, T. F. Antokhina, V. I. Sergienko, *Koord. Khim.* **1992**, *18*, 129–132.
[20] I. N. Flerov, M. S. Molokeev, N. M. Laptash, A. A. Udovenko, E. I. Pogoreltsev, S. V. Mel'nikova, S. V. Misyul, *J. Fluorine Chem.* **2015**, *178*, 86–92.
[21] R. Pöttgen, T. Gulden, A. Simon, *GIT Labor-Fachz.* **1999**, *43*, 133–136.
[22] G. M. Sheldrick, *Acta Crystallogr.* **2008**, *A64*, 112–122.
[23] G. M. Sheldrick, *Acta Crystallogr.* **2015**, *C71*, 3–8.
[24] L. J. Farrugia, *J. Appl. Crystallogr.* **2012**, *45*, 849–854.
[25] M. J. Durand, J. L. Galigne, A. Lari-Lavassani, *J. Solid State Chem.* **1976**, *16*, 157–160.
[26] V. T. Deshpande, *Acta Crystallogr.* **1961**, *14*, 794.
[27] N. E. Brese, O'Keeffe, *Acta Crystallogr.* **1991**, *B47*, 192–197.
[28] I. D. Brown, D. Altermatt, *Acta Crystallogr.*, **1985**, *B41*, 244–247.
[29] R. Hoppe, S. Voigt, H. Glaum, J. Kissel, H. P. Müller, K. Bernet, *J. Less-Common Met.* **1989**, *156*, 105–122.
[30] M. Nespolo, B. Guillot, *J. Appl. Crystallogr.* **2016**, *49*, 317–321.